Journal of Power Sources 195 (2010) 6280–6286

Contents lists available at ScienceDirect

Journal of Power Sources

journal homepage: www.elsevier.com/locate/jpowsour

The impact of flow distributors on the performance of planar solid oxide fuel cell

C.M. Huang[a], S.S. Shy[a,b,*], H.H. Li[a], C.H. Lee[c]

[a] Department of Mechanical Engineering, National Central University, 300 Jhong-da Road, Jhong-li, Tao-yuan 32001, Taiwan
[b] Center for Energy Research, College of Engineering, National Central University, Taiwan
[c] Institute of Nuclear Energy Research, Lung-tan, Tao-yuan 32546, Taiwan

ARTICLE INFO

Article history:
Received 25 February 2010
Received in revised form 22 April 2010
Accepted 22 April 2010
Available online 18 May 2010

Keywords:
Planar solid oxide fuel cell
Single-cell stack test
Flow distributors
Flow uniformity
Cell performance measurements
Anodic re-oxidation

ABSTRACT

This paper presents a newly established testing rig for planar solid oxide fuel cell. Two sets of nearly identical single-cell stacks except using different designs of flow distributors are measured to show how exactly the cell performance of such single-cell stacks would vary with a change in the degree of flow uniformity. It is found that by using small guide vanes around the feed header of commonly used rib-channel flow distributors to improve effectively the degree of flow uniformity, the power density of the single-cell stack can be increased by 10% as compared to that without using guide vanes under exactly the same experimental conditions. Also discussed are the start-up procedure and effects of hydrogen and air flow rates varying from 0.4 slpm to 1 slpm on cell performance of these two single-cell stacks which are measured over a range of the operating temperature varying from 650 °C to 850 °C. After 100 h of continuous cell operation, the examination of the reduction and oxidation stability of the anodic surface reveals that the improvement of flow uniformity in flow distributors is useful to achieve a more balanced use of the anodic catalyst.

1. Introduction

The planar solid oxide fuel cell (SOFC) is of great interest because of its fuel flexibility, compactness, and potential for achieving very high power density [1]. A typical planar SOFC is assembled by the positive electrode–electrolyte–negative electrode (PEN) and the current collectors on both anode and cathode sides that are sandwiched by a pair of interconnects or flow distributors. Nowadays, many different designs of interconnects or flow distributors with straight flow channels separated by rectangular ribs have been used to distribute the fuel and the oxidant gases to the PEN surface, see for instances Refs. [2,3] among many others. A typical flow pathway of interconnects in planar SOFCs may include three parts from a feed header and multi-flow channels to an exhaust header. Furthermore, a good design of flow distributors not only can distribute the fuel and the air uniformly onto the anode and the cathode for achieving uniform diffusion processes through porous electrodes, but also can provide sufficient air flow on the cathode for removing possible hot spots during the long-term cell operation. Thus, the optimization of interconnects or flow distributors is crucial for further improvement of the cell performance of planar SOFC [4,5].

Recently, Shy and co-workers [6] found that flow uniformity in rib-channel interconnects may play a role on the cell performance of a single-cell stack based on 3D numerical models. Note that these numerical flow results in Ref. [6] have been validated by experimental flow data measured by a hydraulic platform. In Ref. [6], four different designs of flow distributors with the same 12 rectangular flow channels divided by 11 ribs were investigated, as schematically shown in Fig. 1a. These four designs were respectively (1) a single-inlet/single-outlet design proposed by Yakabe et al. [7], (2) a double-inlet/single-outlet design by de Haart et al. [8], (3) same as (2) but with an extended rib in the center dividing symmetrically these 12 flow channels into two portions, and (4) same as (2) but with 10 small guide vanes equally spaced in the feed header. A flow uniformity coefficient,

$$\Gamma = \left\{ 1 - \left[\frac{1}{n} \sum_{i=1}^{n} \left(\frac{u_i - \bar{u}}{\bar{u}} \right)^2 \right]^{0.5} \right\} \times 100\%,$$

proposed by Huang et al. [6], was used to indicate the degree of flow uniformity for these aforementioned designs of interconnects, where $n = 12$ representing the total number of rib-channels, u_i the flow velocity in the ith rib-channel, and $\bar{u}$ the averaged mean velocity. Both flow simulations and measurements showed that the design (4) using simple guide vanes in the feed header can significantly improve the flow uniformity and thus can provide the most uniform flow distribution among these four different designs [6].

* Corresponding author at: Department of Mechanical Engineering, National Central University, 300 Jhong-da Road, Jhong-li, Tao-yuan 32001, Taiwan.
Tel.: +886 3 426 7327; fax: +886 3 427 6157.
E-mail address: sshy@ncu.edu.tw (S.S. Shy).

0378-7753/$ – see front matter © 2010 Elsevier B.V. All rights reserved.
doi:10.1016/j.jpowsour.2010.04.073

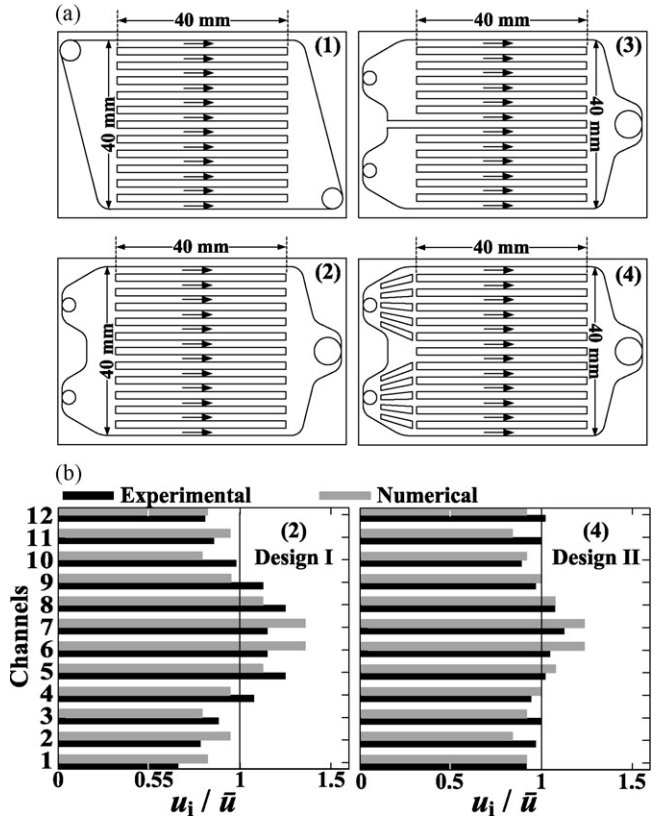

Fig. 1. (a) Schematics of four different designs of flow distributors previously used in numerical studies [6]. (b) Comparisons of experimental and numerical velocity distributions in 12 rib-channels for designs (2) and (4) (here denoted as designs I and II), where $\bar{u}$ was the mean velocity averaged from the velocity data in 12 rib-channels. These velocity data were extracted from Fig. 6 in Ref. [6].

For completeness, flow velocity distributions in each of these 12 rib-channels for the designs (2) and (4) are presented in Fig. 1b, both including experimental and numerical data extracted from Fig. 6 of Ref. [6]. Note that here we denote these two previous designs (2) and (4) as the designs (I) and (II). It can be seen that by using simple small guide vanes evenly spaced in the feed header (design II), the degree of flow uniformity can be significantly improved where the value of Γ is greater than 90% as compared to that of design I without using small guide vanes where $\Gamma \approx 80\%$. More important, such improvement on the degree of flow uniformity can result in an increase of the peak power density (PPD) up to 11% as suggested in Ref. [6] based on 3D numerical models. This motivates the present work aiming to address the following question. How exactly would the effect of flow uniformity vary with a change in the power density of single-cell stacks using different designs of flow distributors? Hence, this paper introduces a high-temperature SOFC testing rig to measure the cell performance for these aforementioned single-cell stacks. By comparing the power-generating characteristics between two sets of nearly identical single-cell stacks except that different designs of flow distributors (designs I and II) having different degrees of flow uniformity are applied, the influence of flow uniformity to cell performance can be thus measured. However, there are some problems to be solved before a clear-cut result on the effect of flow uniformity can be obtained, as discussed below.

At high-temperature conditions, the commonly used metallic interconnects using the materials such as the chromium-based (Cr) alloy with a higher oxidant resistance (e.g. crofer 22-APU) and the doped $LaCrO_3$-based ceramics have higher values of the coefficient of thermal expansion (CTE) than that of the PEN, resulting in high thermal stresses and probably causing cracks of the PEN [9]. Furthermore, the Cr-based vapor species volatilized from these metallic interconnects can be oxidized and deposited on the cathode, which in turn inhibit the reduction of oxygen when the operating temperature is higher than 800 °C [10]. Both the mismatch of CTE among components and the Cr-poisoning problems can lead to rapid cell degradation [11]. To circumvent the aforementioned problems, Liu et al. [12] established a single-cell stack using a disc-shape PEN. In Ref. [12], the gaseous reactants were distributed via various pin-type ceramic flow distributors and the current on the surface of electrodes was directly collected by Ni (anode) or Pt (cathode) meshes, so that the Cr-poisoning problem from the metallic interconnects can be avoided. In addition, the single-cell stack was assembled using a seal-less arrangement and thus the CTE matching problem among various components can be also avoided [12]. It should be noted that such a seal-less assembly could have a serious problem on the cell degradation due to the cross-leakages of fuel and air in the single-cell stack. This leakage problem must be solved before any practical use. Therefore, this study applies the similar methodology proposed by Liu et al. [12] using ceramic rib-channel flow distributors and the seal-less assembly for the present square-shape single-cell stack test, where the currents on the surface of electrodes are collected by using Ni and Pt meshes for the anode and the cathode, respectively. Further, we keep the flow rate of the anode being at least equal to or slightly higher than that of the cathode to avoid the possible air leakage to the anode when the seal-less assembly is used.

In the following sections, we will first introduce the single-cell stack testing rig. Next we will describe the start-up procedure and show the time dependence of the open circuit voltage (OCV) for the present two sets of nearly identical single-cell stacks except using different designs of flow distributors. Results of power-generating characteristics are then presented to demonstrate how exactly the cell performance of these two sets of single-cell stacks would vary with a change in the degree of flow uniformity. Variations of operating temperatures and hydrogen and air flow rates to the cell performance of the single-cell stacks are also discussed. Finally, we will show the observation of the re-oxidation zone on the anodic surface of the PEN after 100 h of the continuous cell operation that occurs only in the case using the design I.

2. A single-cell stack testing rig

Fig. 2 shows photographs of a SOFC testing platform using a temperature-controlled furnace where the single-cell stack is tested. Also shown in Fig. 2 are various gas supply lines, the humidifier, the flow controller, the monitoring and measuring system (a Prodigit 3310D electronic load controlled by a data acquisition computer), and an exhaust gas hood. The furnace can provide an isothermal environment from room temperature to 1000 °C. Thus, the current–voltage (I–V) and current–power (I–P) characteristics of the single-cell stack can be measured at the selected high-temperature conditions.

The left part of Fig. 3 presents a photograph of the arrangement of the testing single-cell stack embedded in a ceramic housing inside a furnace, whereas the right part shows the exploding sketch of such a single-cell stack. As can be seen, the single-cell stack consists of an anode-supported PEN with an effective area of 40 mm × 40 mm (ASC 3 purchased from H.C. Starck), a crofer 22-APU supporting frame, and two current collectors using a porous nickel sponge on the anode side and a platinum mesh on the cathode side for the collection of the electrode current. The use of the metallic frame not only provides the mechanical support to the PEN but also features as a separator to prevent the possible cross-leakages between fuel and oxidant from both feed and

Fig. 2. A SOFC testing platform including a furnace in which the single-cell stack is tested, various gas supply valves and lines, the exhaust gas hood, and power measuring devices.

exhaust headers. In this study, both upper and lower flow distributors (see Fig. 3) are fabricated by aluminum oxide materials, so that the poisoning problem of the electrodes due to the chromium volatilization from the metallic flow distributors can be avoided. The PEN, the frame, and the current collectors are then sandwiched by the upper and lower flow distributors. After many tests, appropriate load plates having a total of 3 kg are applied (see the left part of Fig. 3) in order to obtain a good electrical contact among the PEN and the two current collectors. Note that no bolts are used for the assembly of the present seal-less single-cell stack. So the stack is not tightly screwed and thus the CTE matching problem among different components of the stack can be eliminated. The above arrangements are essential to simplify the very complex poisoning and CTE matching problems occurred in the real SOFC operation and thus allow a clear-cut measurement purely on the effect of flow uniformity to the cell performance to be achieved. By direct comparing power-generating characteristics between two sets of nearly identical single-cell stacks except using different designs of flow distributors, one with small guide vanes around the feed header having higher flow uniformity (design II) and the other without (design I), we are able to identify the actual influence of flow uniformity to the cell performance.

3. The start-up procedure

The standardization of the testing procedure is crucial to obtain repeatable and reliable experimental data and thus must be taken with great caution. This study follows the same testing procedure proposed by Haanappel and Smith [13] for cell performance measurements of these aforementioned single-cell stacks using

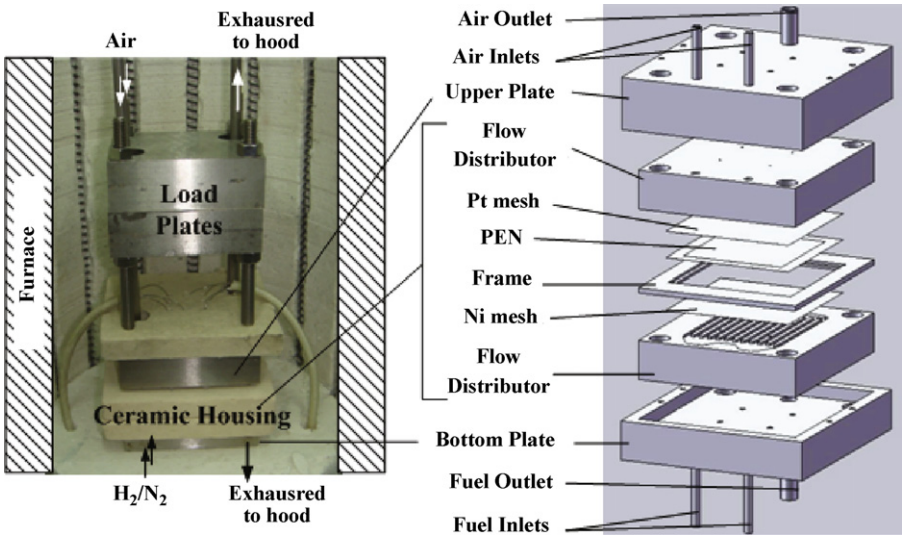

Fig. 3. The arrangement of a testing single-cell stack positioned inside a ceramic housing in the furnace with appropriate loading plates along with the exploding sketch of the single-cell stack.

two different designs of flow distributors. As can be found in Ref. [13], the procedure begins by delivering the test plan and identifying the critical parameters for the cell tests. Following that the single-cell stack is properly mounted to the testing platform for pre-conditioning of the single-cell stack. Then the very slow heating process of the single-cell stack is carried out under nitrogen, cathode and anode sides, respectively, with gas flow rates of 0.2 standard liters per minute (slpm) on both sides [13]. In this study, a programmable logic controller is used to control the temperature of the furnace, such that both heating and cooling rates of the furnace can be controlled at a constant rate of 1 °C min^{-1} in order to very slowly heat up and/or cool down the furnace to the wanted temperature. As pointed out by Haanappel et al. [14], the lower reduction temperature of the anodic catalyst can result in a lower cell performance having a longer time to reach steady state performance and a much larger scattering of data points. Therefore, for achieving a higher cell performance, this study uses a high reduction temperature at T = 850 °C during the 24-h anode reduction process, in which mixtures of hydrogen and nitrogen with the flow rates of $Q_{H_2} = 0.08$ slpm and $Q_{N_2} = 0.2$ slpm are continuously provided to the anode together with an air flow rate of Q_{air} = 0.08 slpm to the cathode.

Fig. 4 shows the entire time dependence of the cell voltage during the start-up process for two independent sets of nearly identical single-cell stacks except that their flow distributors are different, one with small guide vanes (design II) while the other without (design I). Note that the time origin in Fig. 4 is selected at the time when the very slowly heated single-cell stacks have reached the wanted temperature at T = 850 °C. It is found that values of OCV are essentially the same for both designs only in the very beginning of the start-up process. As the anode reduction time increases further up to 2 h, the value of OCV for the design II quickly increases and approaches its maximum value of about 1.15 V. This time period is much faster than that of the design I which needs more than 9 h of the anode reduction time to reach its maximum OCV value. The reason for such a discrepancy in the time dependence of values of OCV between these two cases is clearly due to the influence of flow uniformity, since almost all experimental conditions used in these two sets of single-cell stacks are the same except that the design II using small guide vanes around the feed header of the rib-channel flow distributor has a higher flow uniformity than that of the design I. From the time variation of the cell voltage during the start-up process (Fig. 4), we conclude that a more uniform reduction of the anodic catalyst can be obtained by improving the flow uniformity in rib-channel flow distributors.

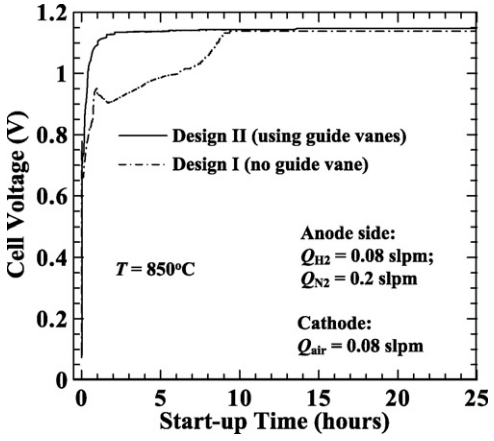

Fig. 4. Variations of OCV during the start-up process for the two sets of identical single-cell stacks except using different flow distributors.

4. Power-generating characteristics

After the completion of the start-up process while keeping the operating temperature constant at T = 850 °C, we measure individually the power-generating characteristics of the aforementioned two single-cell stacks using different designs of flow distributors (designs I and II). For both designs, the measurement begins from the zero current for the OCV and then increases the current density load incrementally, each increment by 12.5 mA cm^{-2}, until that the current density load is increased to be 400 mA cm^{-2}. Furthermore, the measuring time period for each data point should be long enough to assure that the power-generating data are obtained at the equilibrium state. By systematically testing different measuring time periods varying from 0.5 s to 50 s, we found a suitable measuring time period of 30 s that can meet the equilibrium requirement and thus it is used for all measurements in this study. Note that the cell voltage at every incremental step of increasing the current density load is repeatedly measured 30 times to obtain a correct statistical average value. These results are presented and discussed below.

4.1. Effect of flow uniformity at various hydrogen flow rates

Under exactly the same experimental conditions except using or not using 10 small guide vanes in the feed header of flow distributors (see Fig. 1), we measure the I–V and I–P curves for each of two sets of single-cell stacks at four different hydrogen flow rates while keeping $Q_{H_2} = Q_{air}$ and the operating temperature constant at T = 850 °C. These results are presented in Fig. 5, where corresponding values of the power density are also plotted. Our experimental data show that for the case of using small guide vanes (design II), the overall cell performance is found to be generally better than the case without using small guide vanes (design I) and this is valid for all flow rates studied varying from 0.4 slpm to 1.0 slpm. Obviously, such a better cell performance obtained for the design II is due to the usage of small guide vanes that can improve effectively the degree of flow uniformity in rib-channel flow distributors. The higher flow uniformity is, the higher power density is. As seen from Fig. 5a for the case of the lower $Q_{H_2} = 0.4$ slpm, a weak concentration polarization can be observed when the voltage is below 0.7 V. However, for higher hydrogen flow rates (Figs. 5b–d), no sign of the concentration polarization can be observed when the maximum current density load is limited at 400 mA cm^{-2}.

To better demonstrate the effect of flow uniformity to the cell performance, the power density data measured at the maximum current density load (I_d = 400 mA cm^{-2}) for both designs I and II (see Fig. 5) are re-plotted against the hydrogen flow rate. These results are presented in Fig. 6. It is found that at the fixed operating temperature of T = 850 °C, values of the power density, respectively for the design II and/or the design I, increase largely from 259 and/or 232 mW cm^{-2} to 295 and/or 274 mW cm^{-2} when the hydrogen flow rate increases from 0.4 slpm to 0.6 slpm. This result shows that the power density is sensitive to the hydrogen flow rate when $Q_{H_2} \leq 0.6$ slpm. On the other hand, at higher values of $Q_{H_2} = 0.8$ and 1.0 slpm, the power density is found to be not so sensitive to the increase of Q_{H_2}, where the design II has a power density of 311 mW cm^{-2} compared to 280 mW cm^{-2} for the design I at the same $Q_{H_2} = 1.0$ slpm. It is worthy noting that by using simple small guide vanes around the feed header of the rib-channel flow distributor (design II) to improve effectively the degree of flow uniformity, the power density of the single-cell stack can be increased by about 10% as compared to that without using guide vanes (design I) under exactly the same experimental conditions (see Fig. 6).

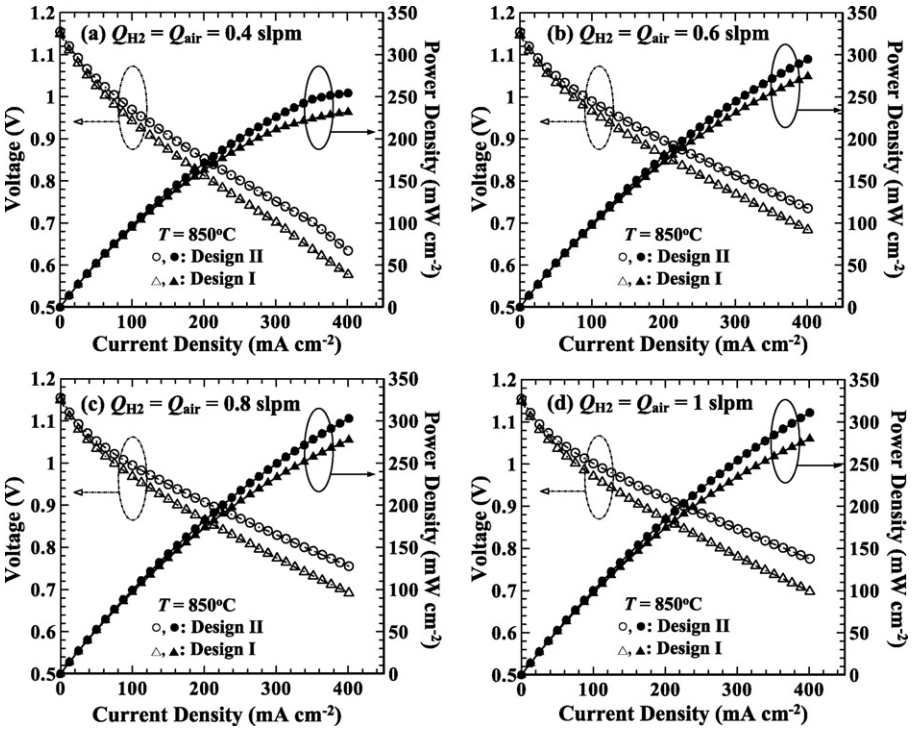

Fig. 5. Comparison of power-generating characteristics between two sets of the single-cell stack using different designs of flow distributors over a range of Q_{H_2} and Q_{air} varying from 0.4 slpm to 1 slpm at a constant operating temperature T = 850 °C.

4.2. Effect of flow uniformity at various operating temperatures

Using the similar arrangement as Fig. 6 for both designs I and II, Fig. 7 presents the comparison of power-generating characteristics between these two single-cell stacks at three different operating temperatures: (a) T = 650 °C, (b) T = 750 °C, and (c) T = 850 °C, respectively, where the flow rates are kept constant at $Q_{H_2} = Q_{air}$ = 1.0 slpm. As can be seen from Fig. 7, values of OCV are about 1.17 V, 1.16 V, and 1.15 V respectively at T = 650 °C, 750 °C, and 850 °C, of which a small decrease of OCV with increasing the operating temperature is found. This is expected because the Gibbs free energy of reactants decreases with increasing temperature. When the operating temperature is low at T = 650 °C, the increase of the power density due to the influence of flow uniformity is only incremental, where the measurement is ended at 0.56 V (Fig. 7a). As T increases, the cell performance for both designs quickly increases because the ionic and electrical conductivities of the cell components increase with the operating temperature. It is found that there is an increase of 11.1% in the value of the power density when compared the design II with the design I at the same T = 850 °C and I_d = 400 mA cm^{-2} (see Fig. 7c). Such an increase in the power density is due to the fact that the higher flow uniformity in flow distributors results in a more uniform use of the anodic catalyst.

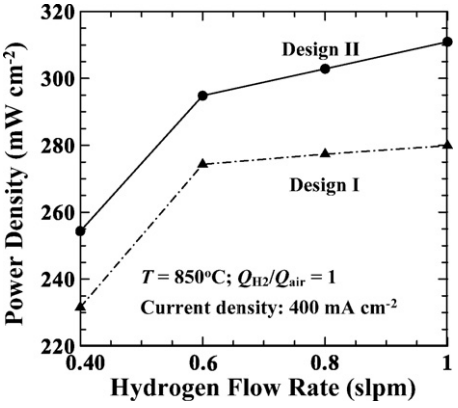

Fig. 6. Effect of hydrogen flow rate on the power density for two sets of identical single-cell stacks except using different flow distributors, where the operating conditions are fixed at T = 850 °C, Q_{H_2}/Q_{air} = 1, and the current density I_d = 400 mA cm^{-2}.

Fig. 8 shows the same power density data measured at 0.8 V from Fig. 7, but plotted against the operating temperature. It is clear that the power density of the design II is very sensitive to the operating temperature, as its value increases from 100 mW cm^{-2} to about 300 mW cm^{-2}, a nearly three-fold increase, when values of T increase from 650 °C to 850 °C. Similar results are also found for the design I. Moreover, the higher the operating temperature is, the larger the influence of flow uniformity is, as can be seen from Fig. 8.

4.3. Observation of anodic re-oxidation zone

Fig. 9a and b presents photographs of two different designs of double-inlet/single-outlet rib-channel flow distributors, respectively the design I and the design II that are used in the aforementioned single-cell stack testing, along with their associated anodic and cathodic surfaces of the PENs after 100 h of the continuous operation. Note that the only difference between these two flow distributors (see Fig. 9) lies in the use of 10 small guide vanes around the feed header for the design II featuring a much higher degree of flow uniformity than that of the design I. Both flow distributors have eight small holes on their rib-channel area allowing the access of the voltage and current probes for power measurements. As seen from Fig. 9a for the design I, different color distributions on the anodic surface of the PEN are observed as marked by white dashed lines, indicating that the anodic catalyst may suffer the formation of anodic re-oxidation zone. This is

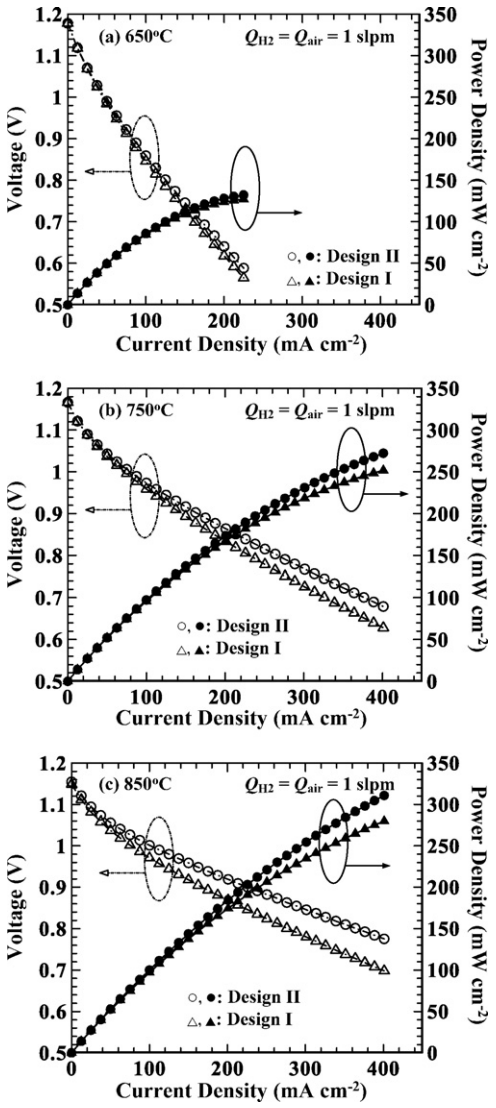

Fig. 7. Comparison of power-generating characteristics between two sets of the single-cell stack using different designs of flow distributors operated at three different temperatures: (a) $T = 650\,^{\circ}C$, (b) $T = 750\,^{\circ}C$ and (c) $T = 850\,^{\circ}C$.

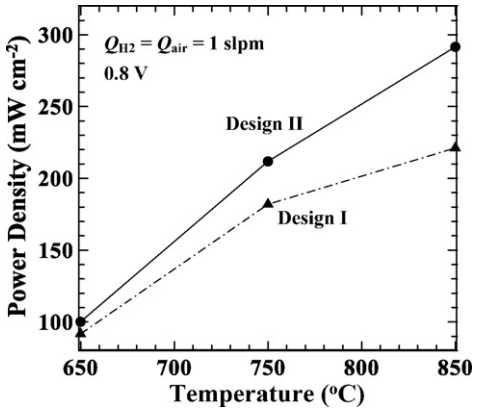

Fig. 8. Effect of operating temperatures on the power density for two sets of identical single-cell stacks except using different flow distributors, in which the comparison is made at the same 0.8 V with $Q_{H_2} = Q_{air} = 1$ slpm.

not due to the air leakage because we have carefully controlled the same flow rates applied for both anode and cathode, and more importantly, the obtained values of OCV are all greater than 1.1 V. In addition, this is not just a one-shot phenomenon, because such an anodic re-oxidation zone is observed for all cases using the design I as their flow distributors after 100 h of cell operation. Previous results applying the scanning electron microscope (SEM) technique have showed that the color of an initial anode (NiO/YSZ) with a stoichiometric ratio between Ni and O elements should be in green, the color of a fully-reduced anode (metallic Ni/YSZ) should be in grey, and the color of a re-oxidized anode ($Ni_{1-\delta}O$/YSZ) should change from green to black (dark green) with increasing δ, as can be found in Ref. [15]. In Fig. 9a, all three colors (green, dark green, and grey) are observed from the anodic surface for the design I. In other words, different composites of the anodic catalyst for the design I have been formed after a long time operation (100 h), on which there are the fully-reduced area (grey color), the local re-oxidized zone (dark green), and the still oxidized part (green). Contrary to that of the design I, only one color of the anodic surface of the PEN is observed when the design II is used, as shown in Fig. 9b, revealing a very uniform reduced anode that is in grey color. By comparing these anodic surfaces between designs I and II, it is straightforward to realize why the better flow uniformity in flow distributors can lead to a better cell performance as discussed in Figs. 5 and 7. To the other side, the cathodic surfaces of the PENs for both designs look almost the same after 100 h of the continuous cell operation (see Fig. 9), probably because the oxygen in the cathode has a much slower reaction rate.

What is the reason for causing the aforesaid anodic re-oxidation in the case of non-uniform flow field? The possible answer may be highlighted from previous studies on the anodic re-oxidation mechanisms (e.g., Refs. [16,17]). As suggested by Hatae et al. [16], the spongy anodic microstructure can be generated when Ni was re-oxidized either by O_2 in air or by the oxide ion current. The latter re-oxidation mechanism has been confirmed by a damage study of Ni–YSZ re-oxidation in anode-supported SOFCs, showing the effect of fuel starvation on the anodic re-oxidation by the oxide ion current. Hence, it is thought that the observed re-oxidation phenomenon occurred only in the case of non-uniform flow field is probably due to local fuel starvation resulting in non-uniform electrochemical reactions and thus non-uniform temperature distributions on the anodic active area.

The aforementioned results are important, because the reduction and oxidation (redox) stability of Ni-based anode is a key reliability issue for SOFCs. The occurrence of the unwanted re-oxidation zone on the anodic surface can decrease the porosity of the anode. This in turn inhibits the fuel diffusion process through the porous anode, makes micro cracks at the interface between the anode and the electrolyte possible, and eventually causes the sever degradation of the anodic catalyst. Such an anodic re-oxidation is attributed to non-uniform fuel flow velocities in these 12 rib-channels (design I), because a non-uniform fuel distribution can result in a non-uniform fuel utilization on the anode and a significant drop of the fuel partial pressure, close to zero, may occur locally for some very small fuel flow velocities. That is why the anodic re-oxidation zone does not occur when the design II with a very high degree of flow uniformity is applied. When the local re-oxidation of the anode occurs, the corresponding local part of the Ni-mesh is also oxidized, which in turn insulates the pass way of the electrons from the anode to the current collector resulting in a decrease of the cell performance. Hence, the improvement of flow uniformity in flow distributors is useful to increase the cell performance (see Figs. 5–8), to avoid the unwanted local re-oxidation of the anode, and to extend the longevity of the cell stack (see Fig. 9).

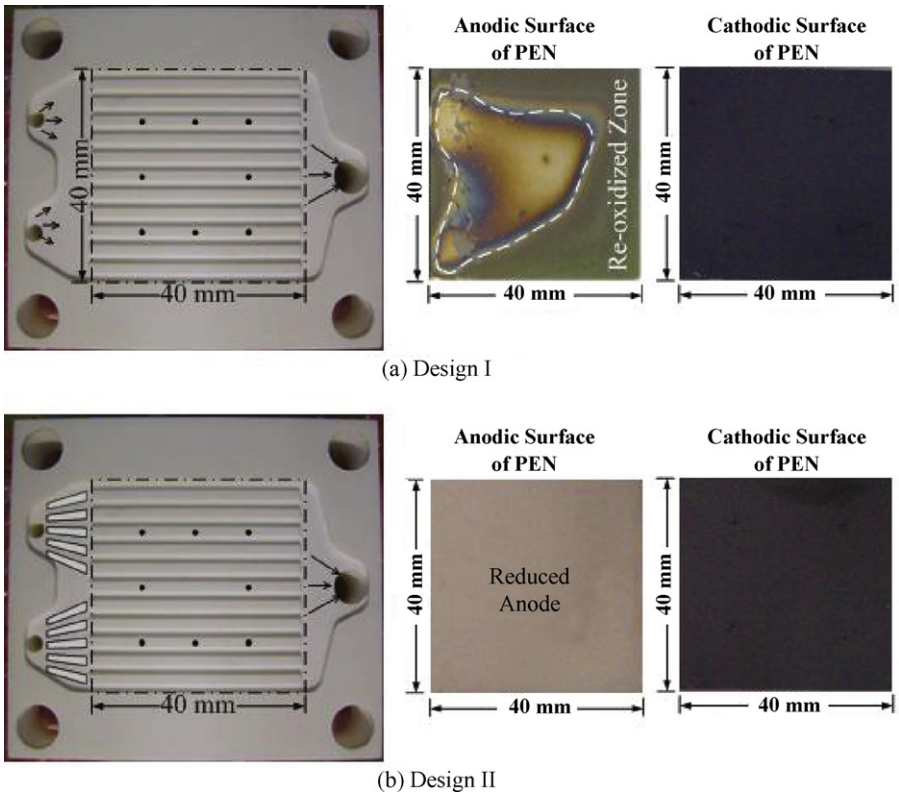

Fig. 9. Two different designs of flow distributors without and/or with guide vanes (designs I and II) and their associated anodic and cathodic surfaces of the PEN after 100 h of operation, showing the influence of flow uniformity on anodic re-oxidation zones occurring only for the case of design I.

5. Conclusions

A high-temperature single-cell stack testing rig for planar SOFC is established to measure the influence of flow uniformity to power-generating characteristics of single-cell stacks over a range of the operating temperature and the hydrogen flow rate. It is found that by simply using small guide vanes equally spaced around the feed header of commonly used rib-channel flow distributors to effectively increase the degree of flow uniformity in flow distributors, the power density of the single-cell stack can be increased by about 10% as compared to that without using guide vanes under exactly the same experimental conditions. Therefore, the present measurement validates our previous numerical predication using the same single-cell stack configuration [6]. Furthermore, the improvement of flow uniformity in flow distributors is helpful to enhance the redox stability of the Ni-based anode, so that a balanced use of the anodic catalyst can be achieved for the continuous cell operation. This is important to extend the longevity of the cell stack.

These results should be useful for planar SOFCs. For further studies, we are currently conducting measurements of resistance spectra of these single-cell stacks using the AC impedance and study the microstructures of the electrodes by SEM in order to understand the cell degradation mechanism and the redox stability of the anode in more depth. These experimental data will be reported in the future.

Acknowledgments

The financial supports from the National Science Council (NSC 97-2212-E-008-085-MY3; 98-2221-E-008-058-MY3; 98-3114-E-008-004) and the Institute of Nuclear Energy Research (972001INER036; 982001INER040) in Taiwan are greatly acknowledged.

References

[1] S.C. Singhal, K. Kendall, High-temperature Solid Oxide Fuel Cells: Fundamentals, Design and Applications, Elsevier Ltd, Kidlington, 2003.
[2] Y. Ji, k. Yuan, J.N. Chung, Y.C. Chen, J. Power Sources 161 (2006) 380–391.
[3] Z. Lin, J.W. Stevenson, M.A. Khaleel, J. Power Sources 117 (2003) 92–97.
[4] T. Ackmann, L.G.J. de Haart, W. Lehert, D. Stolten, J. Electrochem. Soc. 150 (2003) A783–A789.
[5] N. Autissier, D. Larrain, J. Van Herle, D. Favrat, J. Power Sources 131 (2004) 313–319.
[6] C.M. Huang, S.S. Shy, C.H. Lee, J. Power Sources 183 (2008) 205–213.
[7] H. Yakabe, T. Ogiwara, M. Hishinuma, I. Yasuda, J. Power Sources 105 (2001) 144–154.
[8] L.G.J. de Haart, I.C. Vinke, A. Janke, H. Ringel, F. Tietz, in: H. Yokpawa, S.C. Singhal (Eds.), Solid Oxide Fuel Cells (SOFC VII), PV2001-16, The Electrochemical Society Proceedings Series, Pennington, NJ, 2001, p. 111.
[9] A. Selcuk, G. Merere, A. Atkinson, J. Mater. Sci. 36 (2001) 1173–1182.
[10] K. Hilpert, D. Das, M. Miller, D.H. Peck, R. Weiß, J. Electrochem. Soc. 143 (1996) 3642–3647.
[11] H. Tu, U. Stimming, J. Power Sources 127 (2004) 284–293.
[12] H.C. Liu, C.H. Lee, Y.H. Shiu, R.Y. Lee, W.M. Yan, J. Power Sources 167 (2007) 406–412.
[13] V.A.C. Haanappel, M.J. Smith, J. Power Sources 171 (2007) 169–178.
[14] V.A.C. Haanappel, A. Mai, J. Mertens, Solid State Ionics 177 (2006) 2033–2037.
[15] N.M. Tikekar, T.J. Armstrong, A.V. Virkar, J. Electrochem. Soc. 153 (2006) 654–663.
[16] T. Hatae, Y. Matsuzaki, Y. Yamazaki, Solid State Ionics 179 (2008) 274–281.
[17] J. Laurencin, G. Delette, B. Morel, F. Lefebvre-Joud, M. Dupeux, J. Power Sources 192 (2009) 344–352.